

Short communication

Investigation of the heat balance of bipolar NiMH-batteries

J. Harmel^{a,*}, D. Ohms^b, U. Guth^a, K. Wiesener^a

^a Kurt-Schwabe-Institut für Mess- und Sensortechnik Meinsberg e.V, Fabrikstr. 69, Ziegra-Knobelsdorf D-04720, Germany

^b Hoppecke Batterie Systeme GmbH, Brenecketal, Brilon D-59929, Germany

Received 29 July 2004; accepted 21 October 2004

Available online 24 February 2006

Abstract

Heat generation plays an important role for energy storage systems like batteries in electric and hybrid vehicles. In order to investigate the thermal and electrical behaviour the batteries were exposed to cycling programs including various methods of battery cooling by flowing air. Two different experimental methods were presented to study the establishing of the heat balance. The second part of the paper describes the simulation of the temperature distribution by using finite element methods (FEM). The electric and thermal battery model was compared with results obtained from temperature measurements at four selected points during battery cycling.

© 2006 Published by Elsevier B.V.

Keywords: Thermal behaviour; Modelling; Bipolar battery; Metal hydride; Hybrid vehicle; Finite element methods

1. Introduction

The increasing importance of hybrid electric vehicles (HEV) requires an improvement on battery systems. These battery systems must be able to accept or deliver high amounts of power. As volume and weight in a vehicle are rather limited the specific energy and power as well as the energy and power density are important factors for the choice of the battery type. For the use in HEV the ratio of power ability and energy content is favoured. Bipolar stacked nickel metal hydride batteries have demonstrated low internal resistance data and therefore may be candidates for the application as power storage device in HEV [1,2].

As a consequence of the voltage drop caused by any current flow through the battery produces heat. Especially at high currents this heat leads to a local temperature raise. The battery system has to be designed in a way that this quantity of heat can be dissipated and a steady state becomes estab-

lished. Therefore accurate knowledge on the origins of the heat generation is required. As the power requirements are specified by the application the design of the cooling system for the battery has to provide stable working conditions. The design is made difficult by the dependencies of the battery properties on temperature and state of charge (SOC).

A large number of papers point out the necessity of a thermal management for batteries [3,4]. There are several methods to simulate the battery behaviour. Among these computational fluid dynamics (CFD), and finite element methods (FEM) are recommended for the investigation of the thermal systems [5].

Several attempts are made to describe thermal behaviour of batteries during charging but mostly the papers are comparing the simulated data with only one selected position at the battery [6,7]. Our investigations are aimed to make a contribution to the simulation and modelling of batteries during HEV cycling.

For our investigations a 12 V bipolar NiMH stack battery that consists of 10 NiMH sub-cells of a nominal capacity of 1.7 Ah is used. Further details may be found in [1,2].

* Corresponding author.

E-mail address: harmel@ksi-meinsberg.de (J. Harmel).

Table 1
Cycle test program code

Operation	Setting (A)	Limitation value
Charge	0.85	50% C_N
Begin of loop		
Discharge	8.5	10% C_N
Break		2 s
Charge	8.5	10% C_N
Break		2 s
End of loop/number of cycles	100	
Discharge	0.85	10 V

2. Experimental

2.1. Methods

In order to separate the part of power that is dissipated as heat from the battery and the part of power leading to a temperature rise we applied the cycling program displayed in Table 1.

At first the battery is charged to 50% of its nominal capacity with a comparatively small current (0.5 C_N , 0.85 A). Then the battery is cycled in a capacity window of 10% (that is 40–50% SOC) of its nominal capacity with a current of 8.5 A (5 C_N). The time of each charging and discharging step amounts to 72 s and is separated from the next step by a short switching break of 2 s. After 100 cycles the remaining capacity is determined by discharging the battery with a current of 0.85 A (cut-off voltage 10 V).

The experimental set-up is displayed in Fig. 1. The stack under investigation is mounted in one of the three stack positions of a special battery module container. The empty stack positions were blocked in the same way in order to obtain well-defined conditions for the investigation. The module container is equipped with a fan that allows to blow air around the stacks. The air-flow was determined by a laser double anemometer and the temperatures of the air were monitored at the inlet and outlet positions during the experiments.

2.2. Results

The changes of the battery temperature (T_B) during the experiment is shown in Fig. 2. The battery heats up until the 40th cycle and then remains rather constant. As expected the temperature in case of a forced convection is lower than that of the battery left under unforced (natural) convection conditions.

All tests with forced convection lead to rather uniform temperature conditions. The total electric power loss (P_{tot}) of the battery during cycling, given in Fig. 3, declines with increasing battery temperature. This is caused by the reduction of the internal resistance of the electrochemical system at higher temperatures. An increase of the air-flow rate from 210 to 680 min^{-1} does not show any significant influence to the resulting battery temperature.



Fig. 1. Module container (with an empty stack position).

If the energy efficiency is lower than unity the internal electric power loss (P_{tot}), is transferred to a heat increasing the temperature of the battery or is dissipated as heat flow to the surrounding. At higher stack temperatures the heat flow to the surrounding increases due to the larger temperature difference between battery and the adjacent air. The heat dissipation can be enhanced by forcing the air-flow around the battery.

In order to describe the establishing of steady-state conditions two different approaches may be used. For easy computation calculation all energy transfers (and heat flows) are

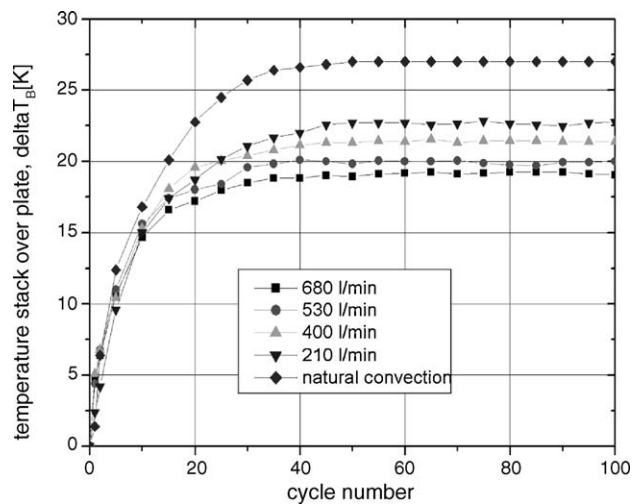


Fig. 2. Battery temperature during cycling (charge/discharge pulses 8.5 A).

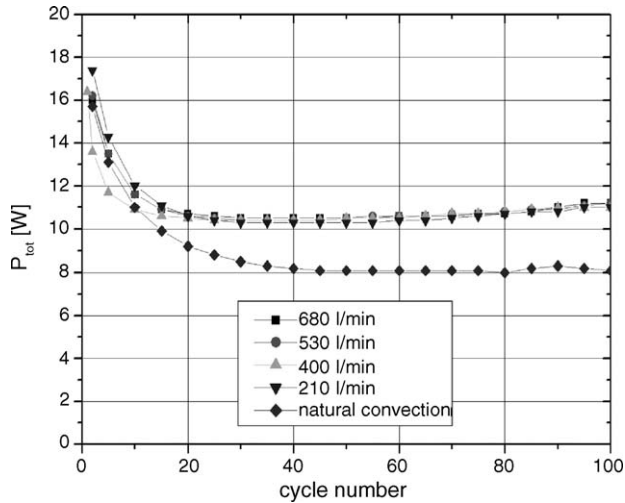


Fig. 3. Total power loss during cycling (charge/discharge pulses 8.5 A).

expressed as power and compared to the electric power loss in the battery.

The first method is based on the determination of the power that heats the internal parts of the battery (P_{remain}). This requires exact knowledge of the heat capacity of the battery.

The second method uses the temperature increase of the coolant (streaming air). It is assumed that all of the heat flow from the battery is being absorbed from the air only and not by other materials. Knowing temperature rise, flow-rate and heat capacity of the air allows to compute the power for that process (P_{diss}).

2.2.1. Computation method 1

The required heat capacity of the battery was determined separately by means of a special adiabatic calorimeter to 760 J K^{-1} .

The equations for the calculation of the total power loss are given by:

$$P_{tot} = \frac{E_{ch} - E_{dch}}{t_{cycle}} \quad (1)$$

$$\Delta T_B = T_{B,i} - T_{B,i-1} \quad (2)$$

$$P_{remain} = \frac{\Delta T_B C_{p,B}}{t_{cycle}} \quad (3)$$

$$P_{diss} = P_{tot} - P_{remain} \quad (4)$$

t_{cycle} is the duration of a cycle, i the index, E_{ch} the charged energy per cycle, E_{dch} the discharged energy per cycle, $C_{p,B}$ the heat capacity of battery, T_B the measured battery temperature, ΔT_B the temperature increase per cycle, P_{remain} the power that heats the battery, P_{diss} the power to be dissipated from the battery as heat, and P_{tot} is the total power loss.

As a consequence of the growing temperature gradient between battery and ambient the power dissipated as heat increases with the number of cycle (Fig. 4). As a consequence

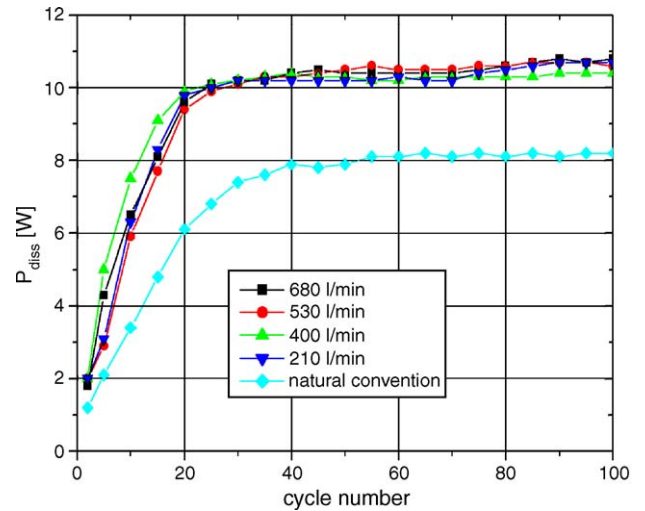


Fig. 4. Power dissipated as heat vs. cycle number (charge/discharge current 8.5 A), method 1.

the power leading to internal heating declines, respectively (Fig. 5). At the beginning of the experiment the complete power loss remains in the battery. At the end, with reaching a steady state at approximately the 40th cycle the power is completely dissipated to the surrounding.

2.2.2. Computation method 2

The second way of the interpretation of data is based on the increase of the temperature of the air flowing around the battery. Using the heat capacity of the air and its flow-rate one is able to compute the portion of power loss removed as heat from the battery. The calculation makes use of the following equations:

$$P_{tot} = \frac{E_{ch} - E_{dch}}{t_{cycle}}$$

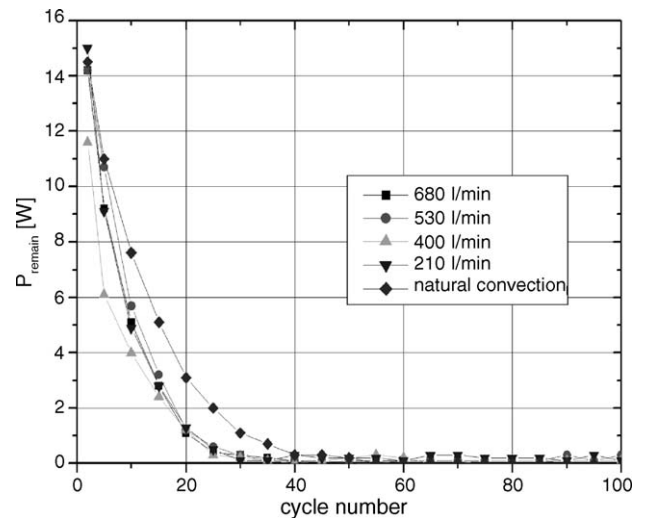


Fig. 5. Power of internal heating vs. cycle number (charge/discharge current 8.5 A), method 1.

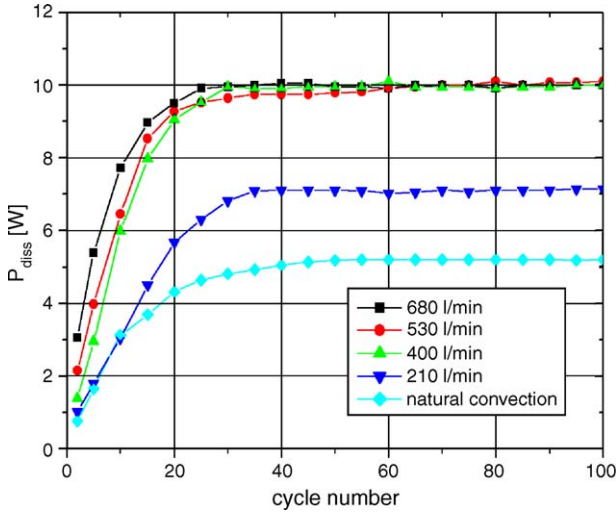


Fig. 6. Power leading to heat dissipation vs. cycle number (charge/discharge 8.5 A), method 2.

$$\Delta T_{\text{air}} = T_{\text{air-off}} - T_{\text{air-on}} \quad (5)$$

$$P_{\text{diss}} = \frac{\Delta T_{\text{air}} C_{p,\text{air}} v_{\text{air}} \rho_{\text{air}}}{t_{\text{cycle}}} \quad (6)$$

$$P_{\text{remain}} = P_{\text{tot}} - P_{\text{diss}} \quad (7)$$

t_{cycle} is the duration of a cycle, ρ_{air} the specific gravity of air (1.29 kg m^{-3}), $C_{p,\text{air}}$ the specific heat capacity from air ($1010 \text{ J kg}^{-1} \text{ K}^{-1}$), ΔT_{air} the difference of temperatures (inlet–outlet), v_{air} the flow-rate of air, P_{remain} the power heating up the battery, P_{diss} the power dissipated as heat, and P_{tot} is the total power loss.

At the beginning there is no heat dissipation from the battery. During the experiment the amount of heat flow is increasing and reaches after 40 cycles an almost constant value (Fig. 6). Finally the complete power loss is being removed

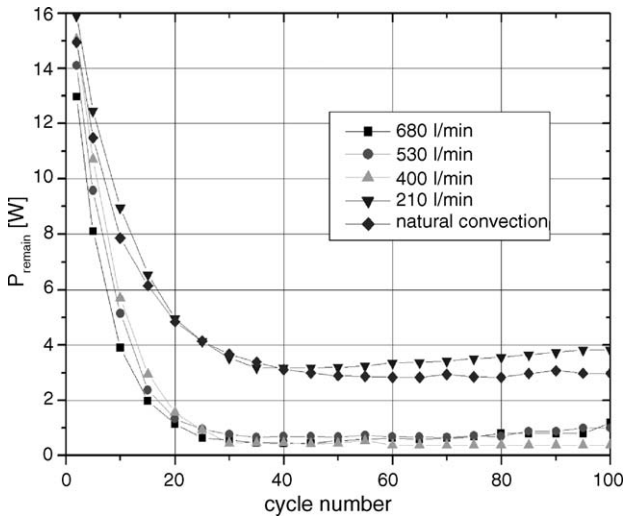


Fig. 7. Power leading to a temperature raise of the battery vs. cycle number (charge/discharge 8.5 A), method 2.

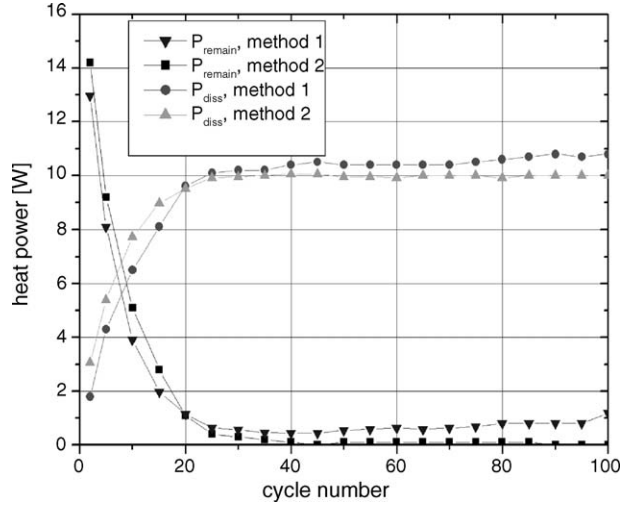


Fig. 8. Comparison of both computation methods.

by the air-flow and the temperature of the battery remains constant (Fig. 7). The deviations observed when using an air-flow rate of 210 l min^{-1} can be explained by the assumption that under the condition of the relatively slow air-flow the battery container will also absorb heat to a certain extent.

2.2.3. Comparison

The two methods are in good agreement with each other (Fig. 8) and may be used to describe the thermal behaviour of the battery.

3. Modelling

3.1. Modelling methods

The finite element method (FEM) is a relatively new simulation method for temperature field and coupled field modelling. The software package ANSYS (a commercial software package to solve FEM problems) offers support for the analysis of fields with coupled physical parameters. In general one can distinguish four steps of FEM analysis [8]:

1. simplification,
2. pre-processing,
3. solution, and
4. post-processing.

The problem was approached by means of a three-dimensional transient electric-thermal model analysis. In the phase of pre-processing a geometric model (meshing) of the battery was built (Fig. 9). The components of the battery were described by their material properties such as specific gravity, heat capacity, heat conductivity, and specific electric resistivity. Thermal conductivity and internal specific resistance of battery stack were measured. The data of specific gravity, thermal capacity and thermal conductivity of the components are based on literature data.

The measuring positions at the battery are indicated. For solution of the model equations the degrees of freedom of

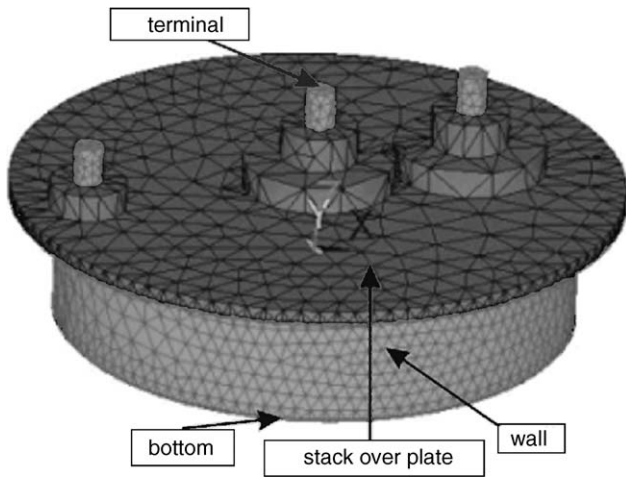


Fig. 9. Three-dimensional geometric battery model (1.7 Ah, 10 sub-cells), with mesh and four measuring (temperature check) points.

voltage and temperature were coupled (multi-physics analysis). Furthermore the electric and thermal loads were applied to the sub-cells.

The heat of absorption and the reversible heat were determined in previous experiments. For the surfaces of the battery natural convection was assumed. The heat transfer data were estimated by application of the data of the VDI-Wärmeatlas [9].

The results of modelling can be visualised and compared to measured data.

3.2. Modelling results

3.2.1. Charge with 5C current (8.5 A)

At first the charging process with 5C rate was modelled. The resulting temperature distribution is visualised in Fig. 10. The top of the battery displays the highest temperatures. This can be explained by the short distance and good thermal connection to the electrode package in the stack. The bottom and the side walls show comparatively low temperatures. In Fig. 11 the good agreement of the results of calculation and

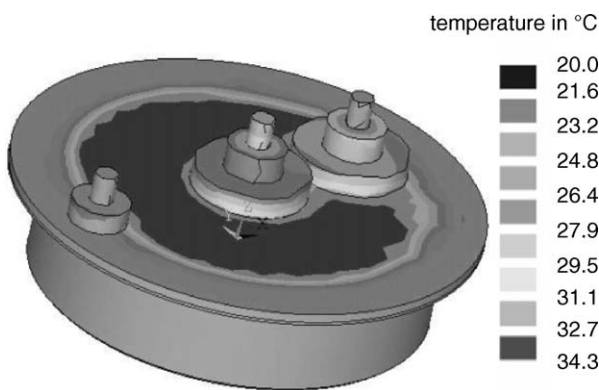


Fig. 10. Temperature distribution of the battery model at the end of charge (8.5 A).

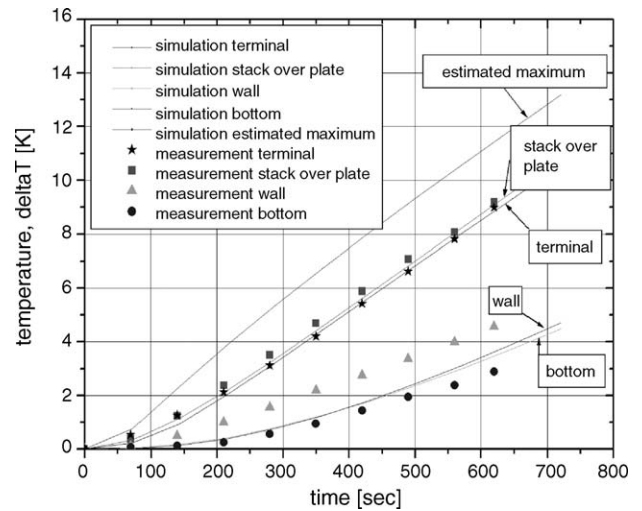


Fig. 11. Temperature distribution of the battery (experimental and calculation) at the end of charge (8.5 A).

experiment are shown. The advantage of the model consists in the information on the internal temperature distribution. Thus the position and magnitude of the maximum temperature can be guessed.

3.2.2. Cycling with 5C current (8.5 A)

As next step a complete cycle was simulated for the NiMH-battery. Charge and discharge were separated from each other by a long break of 3 h. That is not a typical hybrid cycle but it allows to test the validity of the assumptions for the heat transfer. The results are in good agreement with the experimental data as can be seen in Fig. 12. The model can therefore be used to simulate complete battery cycles.

3.2.3. Simulation of high performance cycling

By means of APDL, a macro-language for ANSYS, even more complex load profiles, as for example the profile given in Section 2.1 can be simulated. The results of the simulation

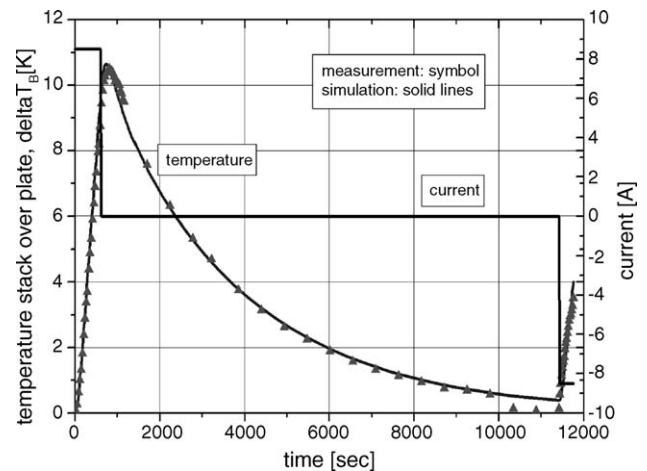


Fig. 12. Temperature of the battery at the top position (experimental and calculation) during a complete cycle (8.5 A).

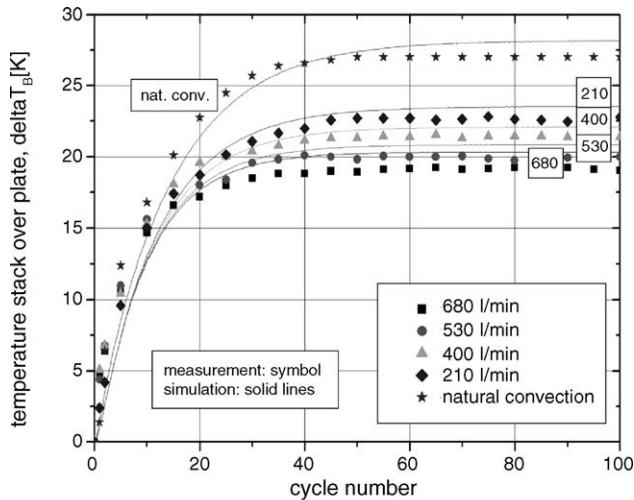


Fig. 13. Temperature on the top of the battery (experimental and calculation) during a high current cycle (8.5 A).

and the experiment are compared in Fig. 13. The good agreement between simulation and experiment demonstrates that the assumption in Section 3.1 was useful and the method can be applied to describe the thermal behaviour of the batteries in hybrid applications.

4. Conclusion

It was shown that the power loss and the heat dissipation will lead to a steady-state condition. The dynamic behaviour

of the battery can be described by a thermal and electric FEM model, in good agreement with the experimental findings. The model allows to make statements on the internal temperature distribution and may also be applied for complete battery cycles.

Acknowledgements

We want to acknowledge for financial support by the German Ministry of economy (BMWA) under contract ERG-0329910G.

References

- [1] D. Ohms, M. Kohlase, G. Benczúr-Ürmösy, K. Wiesener, J. Harmel, *J. Power Sources* 105 (2002) 120–126.
- [2] D. Ohms, M. Kohlase, G. Benczúr-Ürmösy, G. Schädlich, K. Wiesener, J. Harmel, *J. Power Sources* 96 (2001) 76–84.
- [3] A. Grabowski, A.K. Jaura, E. Jih, Efficient cooling and package of traction battery in hybrid electric vehicles, in: *Proceedings of the EVS 18*, Berlin, 2001.
- [4] D.Y. Jung, B.H. Lee, S.W. Kim, *J. Power Sources* 109 (2002) 1–10.
- [5] B.Y. Liaw, K.P. Bethune, X.G. Yang, *J. Power Sources* 110 (2002) 330–340.
- [6] H. Maleki, A.K. Shamsuri, *J. Power Sources* 115 (2003) 131–136.
- [7] A.A. Pesaran, *J. Power Sources* 110 (2002) 377–382.
- [8] C. Groth, G. Müller, *FEM für Praktiker—Temperaturfelder*, Expert Verlag, Renningen-Malmsheim, 1998, pp. 102–107.
- [9] Verein Deutscher Ingenieure, *VDI-Wärmeatlas*, Springer-Verlag, Berlin, 1997.